

Localization of the Centre of the Highest Region of the Triceps Brachii Muscle Spindle Abundance and its Significance in Muscle Spasticity Block

Localización del Centro de la Región más Alta del Huso del Músculo Tríceps Braquial y su Importancia en el Bloqueo de la Espasticidad Muscular

Xiaojiao He¹; Yanrong Li²; Jie Wang³; Shuangjiang Hu²; Meng Wang¹ & Shengbo Yang¹

HE, X.; LI, Y.; WANG, J.; HU, S.; WANG, M.; YANG, S. Localization of the centre of the highest region of the triceps brachii muscle spindle abundance and its significance in muscle spasticity block. *Int. J. Morphol.*, 40(4):1100-1107, 2022.

SUMMARY: This study aimed to accurately localize the location and depth of the centre of the highest region of muscle spindle abundance (CHRMSA) of the triceps brachii muscle. Twenty-four adult cadavers were placed in the prone position. The curve connecting the acromion and lateral epicondyle of the humerus close to the skin was designed as the longitudinal reference line (L), and the curve connecting the lateral and the medial epicondyle of the humerus was designed as the horizontal reference line (H). Sihler's staining was used to visualize the dense intramuscular nerve region of the triceps brachii muscle. The abundance of muscle spindle was calculated after hematoxylin and eosin stain. CHRMSA was labelled by barium sulphate, and spiral computed tomography scanning and three-dimensional reconstruction were performed. Using the Syngo system, the projection points of CHRMSA on the posterior and anterior arm surface (P and P' points), the position of P points projected to the L and H lines (PL and PH points), and the depth of CHRMSA were determined. The PL of the CHRMSA of the long, medial, and lateral heads of the triceps brachii muscle were located at 34.83 %, 75.63 %, and 63.93 % of the L line, respectively, and the PH was located at 63.46 %, 69.62 %, and 56.07 % of the H line, respectively. In addition, the depth was located at 34.73 %, 35.48 %, and 35.85 % of the PP' line, respectively. These percentage values are all the means. These body surface locations and depths are suggested to be the optimal blocking targets for botulinum toxin A in the treatment of triceps brachii muscle spasticity.

KEY WORDS: Triceps brachii muscle; Muscle spasticity; Intramuscular nerve; Muscle spindle; Target localization.

INTRODUCTION

The triceps brachii muscle consists of the long, medial, and lateral head, and its main role is to extend the elbow joint, where the long head also has the function of adduction and extension of the shoulder joint (Ali *et al.*, 2015; Landin *et al.*, 2018). Patients with stroke, spinal cord injury, multiple lateral sclerosis, and traumatic brain injury often develop varying degrees of muscle spasticity as their condition progresses. When the triceps brachii muscle is spastic, the flexion of the elbow becomes difficult and the shoulder joint adducts and rotates internally but cannot be abducted (Hefter *et al.*, 2012; Koo *et al.*, 2019). Currently, intramuscular injection of Botulinum Toxin A (BTX-A) is

more commonly used to treat muscle spasticity (Supiot *et al.*, 2018). The mechanism of action of BTX-A is to block acetylcholine release from the presynaptic membrane of the motor endplate, thereby inhibiting muscle excitation (Isner-Horobeti *et al.*, 2016).

However, the staining of motor endplate bands is limited by the collection of fresh specimens. As the intramuscular nerve dense region (INDR) is consistent with the position of the motor endplate band, the research on INDR as an alternative target for BTX-A has become a hot spot (Rha *et al.*, 2016; Wang *et al.*, 2020; Li *et al.*, 2021).

¹ Department of Human Anatomy, Zunyi Medical University, Zunyi 563099, People's Republic of China.

² Department of Radiology, Affiliated Hospital of Zunyi Medical University, Zunyi 563000, People's Republic of China.

³ Department of Pain, Affiliated Hospital of Zunyi Medical University, Zunyi 563000, People's Republic of China.

FUNDING. This work were supported by the National Natural Science Foundation of China (No. 31660294, 31540031); and Science and technology projects of Guizhou Province (No. ZK[2021]-115, ZK[2022]608); and the Guizhou Provincial Health Commission (No. gzwkj2021-277).

The muscle spindle has a high abundance in the INDR and it plays an important role in muscle spasticity, but its distribution is not uniform (Xie *et al.*, 2012). BTX-A is supposed to maximize the block of intrafusal muscle fibres and minimize the effect on extrafusal muscle fibres, which is beneficial to blocking the key link of muscle spasticity (a-g loop) and reducing extrafusal muscle fibres dysfunction (Phadke *et al.*, 2013).

Based on the above background, this study aimed to set the centre of the highest region of muscle spindle abundance (CHRMSA) in the INDR of the triceps brachii muscle as the best target for BTX-A intramuscular injection, thereby improving the target localization efficiency and efficacy in the treatment of triceps brachii muscle spasticity.

MATERIAL AND METHOD

Specimens and ethics. We collected 24 cadavers (12 males and 12 females) of Chinese adults aged 30 to 75 years without a history of neuromuscular disease and upper limb joint deformation. Among them, 12 (6 males; 6 females) were formalin-fixed for intramuscular nerve staining; 12 (6 males; 6 females) were frozen and preserved for hematoxylin and eosin (HE) staining and CHRMSA localization. Specimens were collected and used with the consent of the Ethics Committee of Zunyi Medical University (#2020-1-008).

Gross anatomical observation. With the cadaver in the prone position, a transverse incision was made from the acromion to the superior angle of the scapula, which was then turned downward and continued along the medial edge of the scapula to the inferior angle of the scapula, and turned horizontally outward till the posterior axillary line. The infraspinatus, teres minor muscle, teres major muscle, and part of the deltoid muscle were exposed by turning the skin and subcutaneous fat as one layer from medial to lateral immediately against the muscle surface. A longitudinal incision was then made between the acromion and the lateral epicondyle of the humerus, and a transverse incision was made between the medial and lateral epicondyles of the humerus. The skin and subcutaneous fat were turned medially against the surface of the muscle. The insertions of the teres minor, teres major, and latissimus dorsi muscles were cut off, turned inward to expose the triceps brachii muscle completely, and the number of nerve branches from the radial nerve branches to the three heads of the triceps brachii muscle and the nerve entry points of the muscle were observed.

Design of reference lines. The acromion (point a), the lateral epicondyle of the humerus (point b), and the medial epicondyle of the humerus (point c) were designed as bony landmarks. The curve line close to the skin connecting point a and b served as the longitudinal reference line (L line), and the curve between point b and c served as the horizontal reference line (H line).

Sihler's staining to display intramuscular nerve distribution. The 24 sides triceps brachii muscle of 12 formalin-fixed cadavers (6 males; 6 females) were dissected and processed by the modified Sihler's staining: immersion: 4-5 weeks in 3 % potassium hydroxide + 0.2 % hydrogen peroxide solution; decalcification: 4 weeks in Sihler's I solution (1 part of glacial acetic acid, 2 parts of glycerol, 12 parts of 1 % trichloroacetaldehyde hydrate); staining: Sihler's II solution (1 part of Ehrlich haematoxylin, 2 parts of glycerol, 12 units of 1 % trichloroacetaldehyde hydrate) for 4 weeks; decolourization: Sihler's I solution for 3-18h. The muscle mass was lavender and the nerve branches were black as ideal; neutralization: 0.05 % lithium carbonate solution for 3 h; transparent: 40 %, 60 %, 80 %, and 100 % gradient glycerol for 1 week respectively. The intramuscular nerve distribution was observed on the X-ray reading light box, and photographed. Additionally, the percentage position of the nerve dense region on the muscle length and width was measured by a Vernier calliper.

HE staining and muscle spindle abundance counting. According to the percentage position of nerve dense region on muscle length and width, 12 fresh cadavers were thawed, and the corresponding positions of nerve dense region in the triceps brachii muscle were dissected and cut off. The muscle mass was divided into three equal parts, upper, middle, and lower. They were weighed, fixed by formaldehyde, dehydrated, wax immersed and embedded in paraffin. Successive transverse sections were made, and the slices were 8 μ m in thickness and HE stained. The muscle spindles were observed and reconstructed under a microscope. Once a muscle spindle appeared on the transverse section until it disappeared on the continuous transverse section, the count was one muscle spindle. Following the counting of the number of muscle spindles, the predicted number of muscle spindles was calculated according to the formula $S_{pn}=20.5 m_n^{0.49}$ (S_{pn} , the number of predicted muscle spindles, m_n , muscle weight) (Banks, 2006). Subsequently, the actual number was divided by the predicted number to get the abundance of muscle spindles. The muscle spindle abundance of the three parts was compared and the position of the region with the highest muscle spindle abundance was determined.

Spiral computed tomography(CT) localization of the CHRMSA. The muscle mass of the same size as those used in HE staining of muscle spindles was cut elsewhere in the cadaver and filled in the gaps left by the previous material collection for muscle spindles. Subsequently, the barium sulphate mixed with glue was injected into the CHRMSA and suture was performed in situ layer by layer. Needles were inserted at the body surface landmarks, and a barium sulphate-soaked silk thread was sewn on the reference line between the needles. Spiral CT scanning and three-dimensional reconstruction were performed. Using the Syngo system, the projection points of CHRMSA on the posterior and anterior arm surface were named P and P' points, respectively. Additionally, the intersection point of the vertical line passing through the P point with L line was recorded as the PL point, while the intersection point of the horizontal line passing through the P point with H line was recorded as the P_H point. The length of the curve between the point a and P_L point was recorded as L'. The length of the curve between the point b and PH point was recorded as H'. The percentage position of the CHRMSA on the body surface was determined by calculating $L'/L \times 100\%$ and $H'/H \times 100\%$. On the cross section, the length of P-CHRMSA and PP' was measured, and the CHRMSA percentage depth was determined by calculating $P\text{-CHRMSA}/PP' \times 100\%$.

Statistical processing. All experimental data were processed with SPSS 18.0 software (IBM, USA) and represented as percentages ($\bar{x} \pm s$) % to eliminate the effect of individual differences in height and weight. The measured data were normally distributed; thus, paired t-test was used for data comparison between the left and right sides, an independent sample t-test was used for comparison between men and women, and one-way ANOVA was used for comparison of muscle spindle abundance among different sites. The statistical significance was set at $\alpha=0.05$. $P < 0.05$ was considered as statistically significant.

RESULTS

Gross anatomical findings. The triceps brachii muscle long head branch that originated from the lateral radial nerve mostly emanated from the superior margin level of the teres major muscle, and travelled a distance externally downward and then divided into two branches, of which the upper branch divided into three branches before entering the muscle from the upper part of the long head, and the lower branch did not branch until it entered the muscle from the middle of the long head. Anatomical

findings revealed that approximately 12.5 % (3/24) of the long head muscle branches entered the muscle from the superficial side, and the other 87.5 % (21/24) from the deep side. After the radial nerve sent its long head muscle branch and travelled downward for about 2–3 cm, it sent its internal and external head branch horizontally at the inferior edge of the teres major muscle. The medial and lateral head branch, 33.3 % (8/24), was branched from the medial radial nerve and then divided into the medial and the lateral head branches and entered into the deep or superficial side of the muscle from the beginning end of the two heads. Hence, the medial and lateral head muscle branches emerged as a common trunk. Another 66.7 % (16/24) of the medial and lateral muscle branches of the radial nerve originated from the medial and lateral sides of the radial nerve and entered the muscle from the anterior medial of the original end of the muscle.

Sihler's staining and muscle spindle abundance. The superior branch of the triceps brachii muscle long head branch entered the muscle, travelled laterally, and branched dendritically in the upper one-third of the muscle, and the branches anastomosed with each other to form an intramuscular nerve dense region (INDR1), which was located at the level of $(5.03 \pm 0.37)\%$ to $(18.82 \pm 0.26)\%$ of the length of the muscle belly, with an area of approximately $(5.95 \pm 0.36)\text{ cm}^2$. The inferior branch of the triceps brachii muscle long head branch entered the muscle and travelled outward and downward, with relatively few branches, mainly innervating the muscle fibres in the middle of the muscle belly. The triceps brachii muscle medial head branch entered the muscle and travelled along the long axis of the muscle to reach the insertion end of the muscle, sending arborized branches along the way, which anastomosed with each other to form an intramuscular nerve dense region (INDR2) with an area of about $(5.4 \pm 0.25)\text{ cm}^2$, located at $(57.65 \pm 0.35)\%$ to $(68.81 \pm 0.32)\%$ of the length of the muscle belly. The triceps brachii muscle lateral head branch was divided into two primary branches, the lateral and the medial branch, before entering the muscle (83.33% , 20/24). The lateral primary branch had few branches within the muscle and mainly innervated the upper one-third of the muscle. The medial primary branch branched dendritically in the middle of the muscle belly and formed another intramuscular nerve dense region (INDR3), which was located at the level of $(47.08 \pm 0.26)\%$ to $(63.43 \pm 0.30)\%$ of the length of the muscle belly, with an area of approximately $(7.92 \pm 0.34)\text{ cm}^2$. The middle one-third of the INDR1 and INDR2 and the lower one-third of the INDR3 had the highest abundance of muscle spindle (Fig. 1). The order of the abundance of these three regions in descending order was the middle one-third of INDR1, the middle one-third of

INDR2, and the lower one-third of INDR 3. The spindle abundance within different parts of each INDR is shown in Table I. The difference between the spindle abundance of each part was statistically significant with $P < 0.05$; however, the differences between the spindle abundance of men and women and between left and right sides were not statistically significant with $P > 0.05$ (Table II).

Spiral CT localization of the CHRMSA. The CHRMSA of the long, medial, and lateral heads of the triceps brachii muscle were named CHRMSA1, CHRMSA2, and CHRMSA3, respectively. The percentage positions of PL and PH of each CHRMSA on the L and H lines and the depth of CHRMSA are shown in Table III. There was no significant difference between the left and right sides and

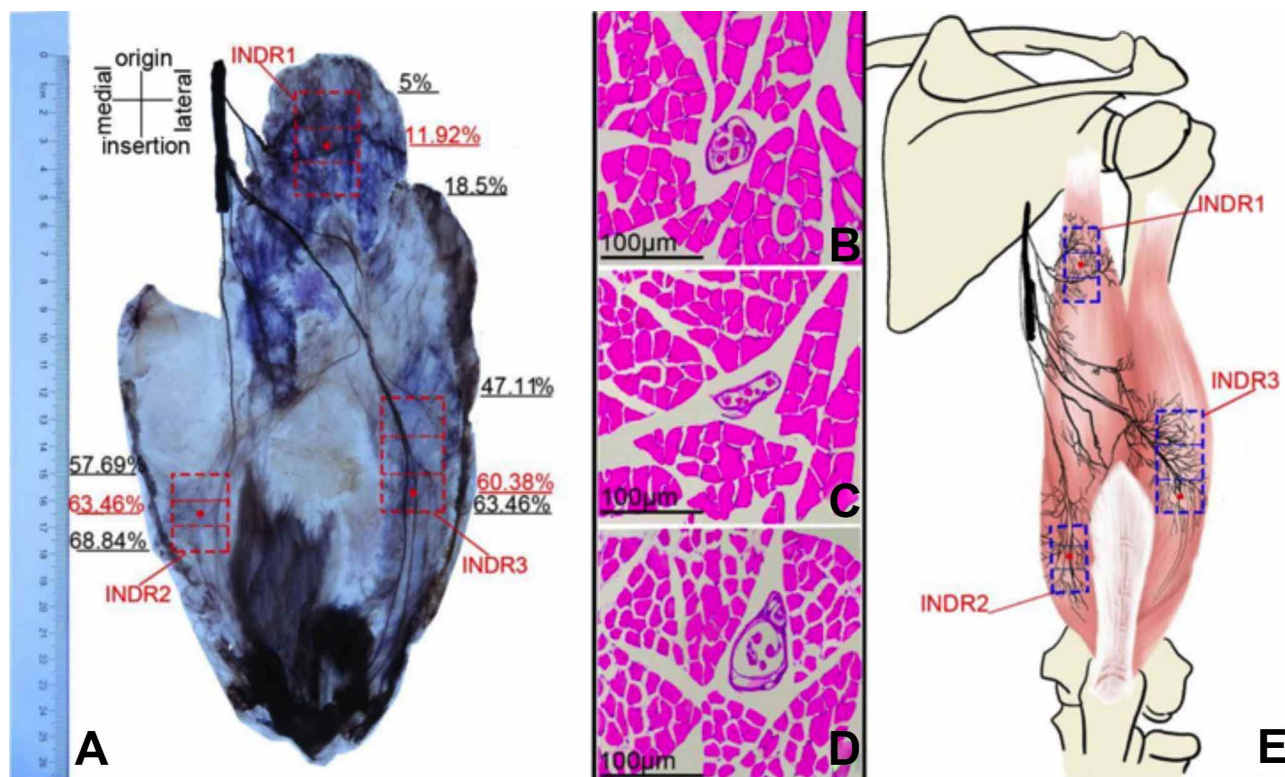


Fig. 1. Sihler's staining of right triceps brachii muscle and the muscle spindle from the region with the highest abundance of muscle spindle. A: Sihler's staining (superficial view). Scale, cm. The red box shows the intramuscular nerve dense region (INDR) location. The red dot in the box indicates the central position of the region with the highest abundance of muscle spindles. B, C, and D are the representative muscle spindles in INDR1, INDR2, and INDR3 of triceps brachii muscle, respectively, which are stained by HE (scale: 100 µm). E: Distribution pattern of intramuscular nerves in the triceps brachii muscle.

Table I. The abundance of muscle spindle in the upper, middle and lower one-third of each INDR in the triceps brachii muscle ($\bar{x} \pm s$)

INDRs	INDR parts	Muscle weight (g)	Actual no.	Predicted no. With correction	Relative abundance
INDR1	Upper one-third	13.08±1.282	16.27±1.033	0.63±0.079	0.8±0.056
	Middle one-third	14.67±1.606	16.37±1.237	0.64±0.098	0.89±0.052
	Lower one-third	12.46±1.560	16.23±1.076	0.62±0.084	0.77±0.103
INDR2	Upper one-third	13.04±1.601	15.22±1.047	0.55±0.075	0.86±0.082
	Middle one-third	14.33±1.308	15.37±1.176	0.56±0.087	0.93±0.048
	Lower one-third	12.50±2.043	15.28±1.076	0.55±0.079	0.82±0.099
INDR3	Upper one-third	12.54±1.817	16.75±1.230	0.67±0.099	0.75±0.082
	Middle one-third	13.54±1.615	17.16±1.199	0.70±0.098	0.79±0.095
	Lower one-third	14.58±1.412	16.95±1.162	0.68±0.093	0.86±0.058

between men and women with $P > 0.05$ (Tables IV, V). The CT image of localization was illustrated by taking the CHRMSA location of the long head of the triceps brachii muscle as an example (Fig. 2).

Table II. Comparison of muscle spindle abundance of each INDR in the triceps brachii muscle between men and women and between the left and right sides.

INDRs	INDR parts	Muscle spindle abundance							
		Male (n=6)	Female (n=6)	<i>t</i>	<i>P</i>	Left side (n=12)	Right side (n=12)	<i>t</i>	<i>P</i>
INDR1	Upper one-third	0.81±0.08	0.80±0.05	0.06	0.952	0.79±0.07	0.82±0.06	-	0.430
	Middle one-third	0.91±0.05	0.88±0.57	1.04	0.307	0.88±0.06	0.90±0.04	-	0.347
	Lower one-third	0.74±0.10	0.80±0.10	-1.34	0.191	0.77±0.11	0.77±0.10	0.1	0.893
INDR2	Upper one-third	0.86±0.09	0.85±0.07	0.20	0.847	0.86±0.09	0.85±0.08	0.2	0.771
	Middle one-third	0.94±0.05	0.92±0.04	1.16	0.257	0.94±0.06	0.93±0.04	0.2	0.772
	Lower one-third	0.84±0.08	0.79±0.11	1.46	0.158	0.81±0.09	0.82±0.11	-	0.857
INDR3	Upper one-third	0.76±0.08	0.73±0.08	0.76	0.454	0.75±0.09	0.74±0.07	0.2	0.829
	Middle one-third	0.78±0.09	0.81±0.10	0.80	0.430	0.77±0.08	0.82±0.10	-	0.224
	Lower one-third	0.87±0.06	0.85±0.06	0.94	0.358	0.87±0.04	0.85±0.07	0.8	0.435

Table III. Percentage positions of PL and PH of each CHRMSA of the triceps brachii muscle on the L and H lines and the percentage depth of CHRMSA ($\bar{x} \pm s$)

CHRMSAs	P _L on line L	P _H on line H	Depth of CHRMSA
	L'/L	H'/H	P-CHRMSA/PP'
CHRMSA1	34.83±2.33	63.46±5.22	34.73±5.27
CHRMSA2	75.63±1.80	69.62±6.87	35.48±4.22
CHRMSA3	63.93±4.35	56.07±9.64	35.85±4.58

Table IV. Comparison of positions of P_L and P_H of each CHRMSA of the triceps brachii muscle on the L and H lines and the percentage depth of CHRMSA between the left and right sides ($\bar{x} \pm s$, %).

CHRMSAs	P _L on line L				P _H on line H				depth of CHRMSA			
	L'/L		<i>t</i>	<i>P</i>	H'/H		<i>t</i>	<i>P</i>	P-CHRMSA/PP'		<i>t</i>	<i>P</i>
	Left side (n=12)	Right side (n=12)			Left side (n=12)	Right side (n=12)			Left side (n=12)	Right side (n=12)		
CHRMSA1	34.23±2.11	35.42±2.46	-1.23	0.233	62.92±5.62	64.00±4.96	-0.51	0.617	34.16±4.85	35.30±5.81	-0.46	0.651
CHRMSA2	76.30±1.96	75.22±1.60	0.99	0.329	69.34±7.04	69.89±7.00	-0.15	0.886	35.07±3.98	35.88±4.59	-0.43	0.672
CHRMSA3	64.01±3.14	63.84±5.44	0.14	0.892	55.43±9.80	56.71±9.80	-0.31	0.758	35.68±4.47	36.01±4.88	-0.09	0.930

Table V. Comparison of positions of PL and PH of each CHRMSA of the triceps brachii muscle on the L and H lines and the percentage depth of CHRMSA between males and females ($\bar{x} \pm s$, %)

CHRMSAs	P _L on line L				P _H on line H				Depth of CHRMSA			
	L'/L		<i>t</i>	<i>P</i>	H'/H		<i>t</i>	<i>P</i>	P-CHRMSA/PP'		<i>t</i>	<i>P</i>
	Male (n=6)	Female (n=6)			Male (n=6)	Female (n=6)			Male (n=6)	Female (n=6)		
CHRMSA1	35.45±1.36	34.83±2.33	1.23	0.233	63.62±6.22	63.46±5.22	0.12	0.908	34.60±6.60	34.73±5.27	-0.15	0.880
CHRMSA2	76.05±1.38	75.63±1.80	0.77	0.450	67.94±7.40	69.62±6.87	-1.17	0.255	35.72±4.28	35.48±4.22	0.24	0.814
CHRMSA3	63.85±2.00	63.93±4.35	-0.14	0.892	53.79±11.72	56.07±9.64	-1.13	0.270	36.21±4.69	35.85±4.58	0.53	0.599

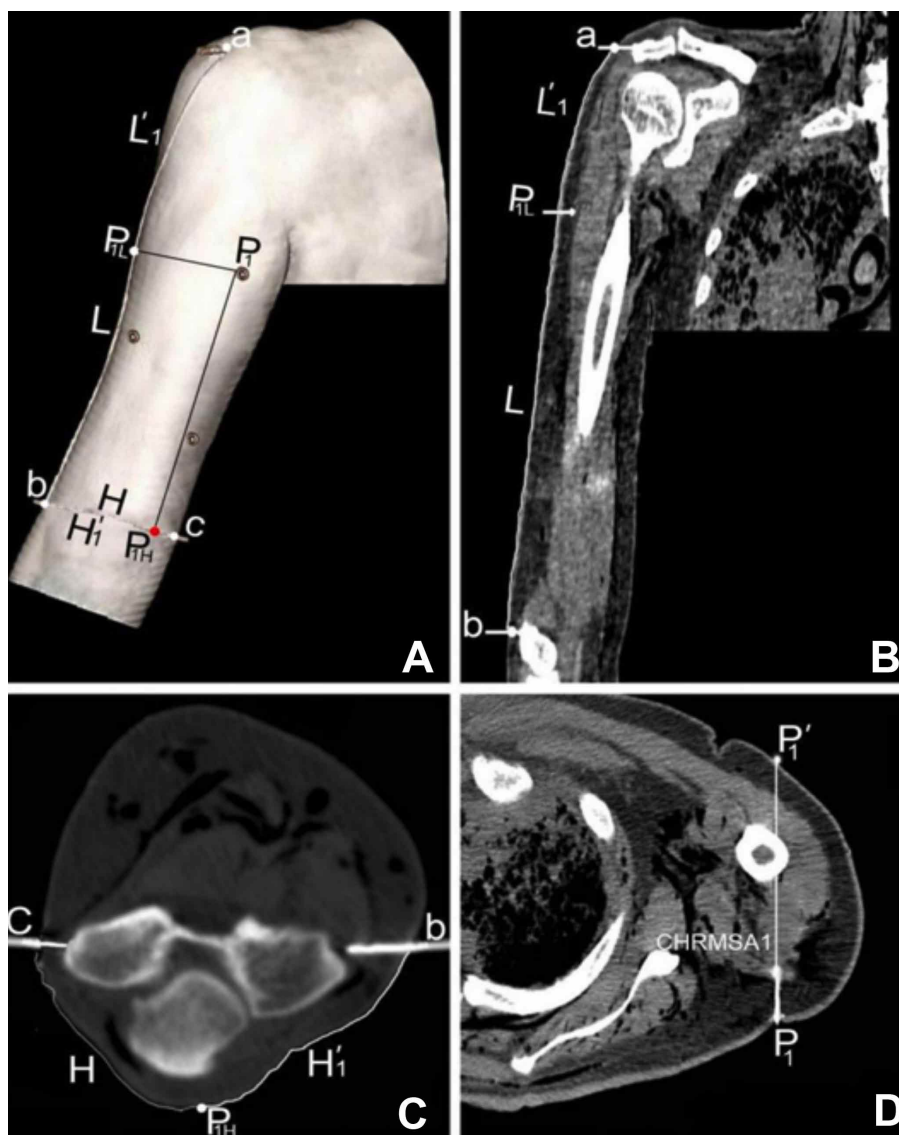


Fig. 2. CT image of CHRMSA localization of the long head of the left triceps brachii muscle. A: Spiral CT three-dimensional reconstruction images show the body surface projection position of CHRMSA1 and the designed reference line. point a, acromion; point b, lateral epicondyle of humerus; point c, medial epicondyle of humerus; P_1 , the body surface projection point of CHRMSA of the long head of the triceps brachii muscle. $ab=L$, $a-P_{1L}=L'$; $bc=H$, $b-P_{1H}=H'$. B: The lengths of L and L' lines are measured on the coronal section through the ab line; C: The lengths of H and H' lines are measured on the cross section through bc line; D: The depth of CHRMSA1 is measured on the cross section through P

DISCUSSION

With the development of medical technology, the number of survivors of central nervous system diseases (Lehoux *et al.*, 2020) has increased, and the number of patients with muscle spasm has increased accordingly. The triceps brachii muscle is the only muscle located at the back of the humerus. It is a double joint muscle (Landin *et al.*, 2018) that participates in the functional activities of both the shoulder and the elbow joints. If the two joints cannot be extended because of their spasms, it will not only affect daily life but also lead to secondary changes in the musculoskeletal system (Nelson *et al.*, 2018) because of its long-term discontinuation. Intramuscular injection of BTX-A is effective in the treatment of muscle spasms, but its

efficacy is closely related to the accurate location of the target. There have been some reports about the innervation source, the position of the nerve branches, and the number of branches of the triceps brachii muscle. Besides the common radial nerve, the nerve to the long head of the triceps brachii muscle can also originate from the axillary nerve (Wade *et al.*, 2018), and the nerve to the medial head can arise from the ulnar nerve (Cho *et al.*, 2019), and there can be 1–3 branches. The autopsy records of Stanescu *et al.* (1996) described that 88 % of the radial nerve innervation of the long head of the triceps brachii muscle originated from the axilla, and 12 % from the brachio-axillary angle. The innervation of the medial head of the triceps brachii muscle

originated from the spiral groove, the brachio-axillary angle, and the axilla in 52 %, 39 %, and 9 % of the patients, respectively. The lateral head of the triceps brachii muscle was innervated by branches arising from the spiral groove, the brachio-axillary, and the axillary branch in 70 %, 24 %, and 6 % of the cases (Stanescu *et al.*, 1996). The above variations were not found in this study. For the distribution of nerve branches in the triceps brachii muscle, an immunohistochemical method has been used to identify whether there are fibres of the ulnar nerve in the medial head (Pascual-Font *et al.*, 2013), but Sihler's staining has not been used to display the overall distribution pattern of intramuscular nerve visible to the naked eye. In this study, the INDR in each head was obtained by Sihler's staining. The muscle spindle was allometric and the muscle spindle abundance of INDR was high according to previous studies (Banks, 2006). Therefore, the INDR was divided into three parts, in which the muscle spindles were counted and the muscle spindle abundance was compared. Additionally, their CHRMSAs were labelled with barium sulphate and scanned by spiral CT to establish the geometric relationship between the CHRMSA and body surface markers, with the expectation to obtain accurate location and depth of BTX-A injection to block triceps spasms. The findings genuinely facilitated the localization of the target on the body surface and revealed its depth and have strong clinical manoeuvrability.

Each head of the triceps brachii muscle has different muscle force and activity patterns at different shoulder elevation angles. When the shoulder joint is barely elevated, the long head contributes more to the elbow extension, and when the shoulder joint is raised 90° or more, the medial head plays a role (Kholinne *et al.*, 2018). This study showed that the muscle spindle abundance in the INDR of the medial head of the triceps brachii muscle was the highest, followed by the long head, then by the lateral head. Therefore, it is suggested that when triceps brachii muscle spasm occurs, the medial head of the triceps can be blocked first, and then the long head or lateral head can be blocked according to the needs of the medical condition. It is reported that 1 unit of BTX-A can infiltrate 1.5–3.0 cm², and 2.5-5.0 units can spread to 4.5 cm² (Wang *et al.*, 2020). Combined with the INDR area measured in this study, the actual BTX-A doses required for long, medial, and lateral head of the triceps brachii muscle are only 1, 1, and 1.5 units, respectively. If the localization is accurate, it reduces the amount of BTX-A and reduces the risk of complications.

In summary, this study revealed the overall distribution pattern of intramuscular nerves in the triceps brachii muscle for the first time, and CHRMSA was designed as the best target for BTX-A injection to block the triceps brachii muscle spasm. Through the combination of gross

anatomy, histological staining, and spiral CT scanning, the body surface location and depth that should be punctured when BTX-A injection is used to block brachii muscle spasm can be accurately located. Since the current study is merely an anatomical study, the findings need to be confirmed in clinical application.

HE, X.; LI, Y.; WANG, J.; HU, S.; WANG, M.; YANG, S. Localización del centro de la región más alta del huso del músculo tríceps braquial y su importancia en el bloqueo de la espasticidad muscular. *Int. J. Morphol.*, 40(4):1100-1107, 2022.

RESUMEN: Este estudio tuvo como objetivo localizar con precisión la ubicación y la profundidad del centro de la región más alta del huso muscular (CHRMSA) del músculo tríceps braquial. Se colocaron veinticuatro cadáveres adultos en posición prona y se designó la curva que conecta el acromion y el epicóndilo lateral del húmero cerca de la piel como la línea de referencia longitudinal (L), y la curva que conecta los epicóndilos lateral y medial del húmero fue designada como la línea de referencia horizontal (H). Se usó la tinción de Sihler para visualizar la región nerviosa intramuscular densa del músculo tríceps braquial. La abundancia de huso muscular se calculó después de la tinción con hematoxilina y eosina. CHRMSA se marcó con sulfato de bario y se realizó una tomografía computarizada espiral y una reconstrucción tridimensional. Usando el sistema Syngo, fueron determinados los puntos de proyección de CHRMSA en la superficie posterior y anterior del brazo (puntos P y P'), la posición de los puntos P proyectados en las líneas L y H (puntos P_L y P_H) y la profundidad de CHRMSA. Los P_L de la CHRMSA de las cabezas larga, medial y lateral del músculo tríceps braquial se ubicaron en el 34,83 %, 75,63 % y 63,93 % de la línea L, respectivamente, y el P_H se ubicó en el 63,46 %, 69,62 %, y 56,07 % de la línea H, respectivamente. La profundidad se ubicó en el 34,73 %, 35,48 % y 35,85 % de la línea PP', respectivamente. Estos valores porcentuales son todas las medias. Se sugiere que estas ubicaciones y profundidades de la superficie corporal son los objetivos de bloqueo óptimos para la toxina botulínica A en el tratamiento de la espasticidad del músculo tríceps braquial.

PALABRAS CLAVE: Músculo tríceps braquial; Espasticidad muscular; Nervio intramuscular; Huso muscular; Localización.

REFERENCES

- Ali, A.; Sundaraj, K.; Badlishah Ahmad, R.; Ahamed, N. U.; Islam, A. & Sundaraj S. muscle fatigue in the three heads of the triceps brachii during a controlled forceful hand grip task with full elbow extension using surface electromyography. *J. Hum. Kinet.*, 46:69-76, 2015.
- Banks, R. W. An allometric analysis of the number of muscle spindles in mammalian skeletal muscles. *J. Anat.*, 208(6):753-68, 2006.
- Cho, S. H.; Chung, I. H. & Lee, U. Y. Relationship between the ulnar nerve and the branches of the radial nerve to the medial head of the triceps brachii muscle. *Clin. Anat.*, 32(1):137-42, 2019.

- Hefter, H.; Jost, W. H.; Reissig, A.; Zakine, B.; Bakheit, A. M. & Wissel, J. Classification of posture in poststroke upper limb spasticity: a potential decision tool for botulinum toxin A treatment? *Int. J. Rehabil. Res.*, 35(3):227-33, 2012.
- Isner-Horobet, M. E.; Muff, G.; Lonsdorfer-Wolf, E.; Deffinis, C.; Masat, J.; Favret, F.; Dufour, S. P. & Lecocq, J. Use of botulinum toxin type A in symptomatic accessory soleus muscle: first five cases. *Scand. J. Med. Sci. Sports.*, 26(11):1373-8, 2016.
- Kholinne, E.; Zulkarnain, R. F.; Sun, Y. C.; Lim, S.; Chun, J. M. & Jeon, I. H. The different role of each head of the triceps brachii muscle in elbow extension. *Acta Orthop. Traumatol. Turc.*, 52(3):201-205, 2018.
- Koo, H. J.; Park, H. J.; Park, G. Y.; Han, Y.; Sohn, D. & Im, S. Safe Needle Insertion Locations for Motor Point Injection of the Triceps Brachii Muscle: A Pilot Cadaveric and Ultrasonography Study. *Ann. Rehabil. Med.*, 43(6):635-41, 2019.
- Landin, D.; Thompson, M. & Jackson M. Functions of the triceps brachii in humans: a review. *J. Clin. Med. Res.*, 10(4):290-293, 2018.
- Lehoux, M. C.; Sobczak, S.; Cloutier, F.; Charest, S. & Bertrand-Grenier, A. Shear wave elastography potential to characterize spastic muscles in stroke survivors: Literature review. *Clin. Biomech. (Bristol, Avon)*, 72:84-93, 2020.
- Li, Y.; Wang, M.; Tang, S.; Zhu, X. & Yang, S. Localization of nerve entry points and the center of intramuscular nerve-dense regions in the adult pectoralis major and pectoralis minor and its significance in blocking muscle spasticity. *J. Anat.*, 239(5):1123-33, 2021.
- Nelson, C. M.; Murray, W. M. & Dewald, J. P. A. Motor impairment-related Alterations in biceps and triceps brachii fascicle lengths in chronic hemiparetic stroke. *Neurorehabil. Neural Repair.*, 32(9):799-809, 2018.
- Pascual-Font, A.; Vazquez, T.; Marco, F.; Sañudo, J. R. & Rodriguez-Niedenführ, M. Ulnar nerve innervation of the triceps muscle: real or apparent? An anatomic study. *Clin. Orthop. Relat. Res.*, 471(6):1887-93, 2013.
- Phadke, C. P.; On, A. Y.; Kirazli, Y.; Ismail, F. & Boulias, C. Intrafusal effects of botulinum toxin injections for spasticity: revisiting a previous paper. *Neurosci. Lett.*, 541:20-3, 2013.
- Rha, D. W.; Yi, K. H.; Park, E. S.; Park, C. & Kim, H. J. Intramuscular nerve distribution of the hamstring muscles: Application to treating spasticity. *Clin. Anat.*, 29(6):746-51, 2016.
- Stanescu, S.; Post, J.; Ebraheim, N. A.; Bailey, A. S. & Yeasting, R. Surgical anatomy of the radial nerve in the arm: practical considerations of the branching patterns to the triceps brachii. *Orthopedics*, 19(4):311-5, 1996.
- Supiot, A.; Geiger, M.; Bensmail, D.; Aegerter, P.; Pradon, D. & Roche, N. Effect of botulinum toxin injection on length and force of the rectus femoris and triceps surae muscles during locomotion in patients with chronic hemiparesis (FOLOTOX). *BMC Neurol.*, 18(1):104, 2018.
- Wade, M. D.; McDowell, A. R. & Ziermann, J. M. Innervation of the long head of the triceps brachii in humans-A fresh look. *Anat. Rec. (Hoboken)*, 301(3):473-83, 2018.
- Wang, J.; Wang, Q.; Zhu, D.; Jiang, Y. & Yang, S. Localization of the center of the intramuscular nerve dense region of the medial femoral muscles and the significance for blocking spasticity. *Ann. Anat.*, 231:151529, 2020.
- Xie, P.; Jiang, Y.; Zhang, X. & Yang, S. The study of intramuscular nerve distribution patterns and relative spindle abundance of the thenar and hypothenar muscles in human hand. *PLoS One*, 7(12):e51538, 2012.

Corresponding author:
Shengbo Yang
Department of Anatomy
Zunyi Medical University
6 West Xufu Road
Xinpu Developing Zones
Zunyi 563099
CHINA

E-mail: yangshengbo8205486@163.com